Biochemical Pharmacology 79 (2010) 1261–1271

Contents lists available at ScienceDirect

Biochemical Pharmacology

journal homepage: www.elsevier.com/locate/biochempharm

Chamaecypanone C, a novel skeleton microtubule inhibitor, with anticancer activity by trigger caspase 8-Fas/FasL dependent apoptotic pathway in human cancer cells

Cheng-Chih Hsieh [a,b], Yueh-Hsiung Kuo [c,d,e], Ching-Chuan Kuo [f], Li-Tzong Chen [f,g], Chun-Hei Antonio Cheung [f], Tsu-Yi Chao [h], Chi-Hung Lin [i,j], Wen-Yu Pan [f], Chi-Yen Chang [f], Shih-Chang Chien [k], Tung-Wei Chen [i], Chia-Chi Lung [f], Jang-Yang Chang [f,g,*]

[a] Graduate Institute of Medical Sciences, National Defense Medical Center, Taipei, Taiwan, ROC
[b] Department of Pharmacy Practice, Tri-service General Hospital, Taipei, Taiwan, ROC
[c] Tsuzuki Institute for Traditional Medicine, College of Pharmacy, China Medical University, Taichung, Taiwan, ROC
[d] Department of Chemistry, National Taiwan University, Taipei, Taiwan, ROC
[e] Agricultural Biotechnology Research Center, Academia Sinica, Taipei, Taiwan, ROC
[f] National Institute of Cancer Research, National Health Research Institutes, Tainan, Taiwan, ROC
[g] Division of Hematology/Oncology, Department of Internal Medicine, National Cheng Kung University Hospital, Tainan, Taiwan, ROC
[h] Division of Hematology/Oncology, Department of Internal Medicine, Tri-service General Hospital, Taipei, Taiwan, ROC
[i] Institute of Microbiology and Immunology, National Yang-Ming University, Taipei, Taiwan, ROC
[j] Institute of Biophotonics Engineering, National Yang-Ming University, Taipei, Taiwan, ROC
[k] School of Chinese Medicine Resources, China Medical University, Taichung, Taiwan, ROC

ARTICLE INFO

Article history:
Received 13 October 2009
Accepted 15 December 2009

Keywords:
Chamaecypanone C
Microtubule inhibitor
Anticancer
Drug resistance
Fas/FasL

ABSTRACT

Microtubule is a popular target for anticancer drugs. Chamaecypanone C, is a natural occurring novel skeleton compound isolated from the heartwood of *Chamaecyparis obtusa* var. *formosana*. The present study demonstrates that chamaecypanone C induced mitotic arrest through binding to the colchicine-binding site of tubulin, thus preventing tubulin polymerization. In addition, cytotoxic activity of chamaecypanone C in a variety of human tumor cell lines has been ascertained, with IC_{50} values in nanomolar ranges. Flow cytometric analysis revealed that chamaecypanone C treated human KB cancer cells were arrested in G_2–M phases in a time-dependent manner before cell death occurred. Additional studies indicated that the effect of Chamaecypanone C on cell cycle arrest was associated with an increase in cyclin B1 levels and a mobility shift of Cdc2/Cdc25C. The changes in Cdc2 and Cdc25C coincided with the appearance of phosphoepitopes recognized by a marker of mitosis, MPM-2. Interestingly, this compound induced apoptotic cell death through caspase 8-Fas/FasL dependent pathway, instead of mitochondria/caspase 9-dependent pathway. Notably, several KB-derived multidrug resistant cancer cell lines overexpressing P-gp170/MDR and MRP were sensitive to Chamaecypanone C. Taken together, these findings indicated that Chamaecypanone C is a promising anticancer compound that has potential for management of various malignancies, particularly for patients with drug resistance.

1. Introduction

Chemotherapy for the treatment of cancer was introduced into the clinic more than fifty years ago. Most chemotherapeutic anticancer drugs used in the clinic today include agents that target the cell cycle in order to inhibit the hyperproliferation state of tumor cells and – subsequently – to induce apoptosis, which is the desired outcome of chemotherapy [1]. Otherwise, the primary hurdle for effective cancer chemotherapy has been the intrinsic or acquired resistance of cancer cells to a variety of anticancer agents

Abbreviations: CA-4, combretastatin A-4; CCD, charge-coupled device; DIC, differential interference contrast; DMSO, dimethyl sulfoxide; FITC, fluorescent isothiocyanate; GFP, green fluorescent protein; HRP, horseradish peroxidase; MAP, Microtubule-associated protein; MDR, multidrug resistance; MRP, multidrug resistance-associated proteins; PI, propidium iodide; SPA, scintillation proximity assay; VP16, etoposide.

* Corresponding author at: National Institute of Cancer Research, National Health Research Institutes, 2F, No. 367, Sheng Li Road, Tainan 704, Taiwan, ROC.
Tel.: +886 6 7000123x65100; fax: +886 6 2083427.
E-mail address: jychang@nhri.org.tw (J.-Y. Chang).

0006-2952/$ – see front matter © 2009 Elsevier Inc. All rights reserved.
doi:10.1016/j.bcp.2009.12.017

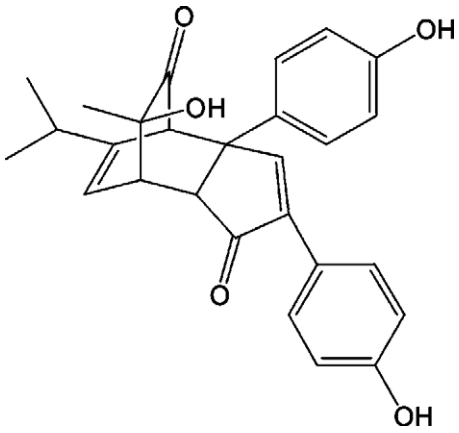

Fig. 1. Chemical structure of Chamaecypanone C.

with distinct chemical structures or mechanism of action, a phenomenon known as multidrug resistance (MDR). The classical form of MDR involves the overexpression of drug efflux transporters such as P-glycoprotien (P-gp170/MDR) and multidrug resistance-associated proteins (MRPs) in the cell membrane, which pump anticancer drugs out of the cells, resulting in low intracellular drug concentrations [2,3]. Therefore, there is necessary to discover the novel chemotherapeutic agents which could overcome MDR.

Historically, plants were a traditional source of medicinal agents. As modern medicine has evolved, numerous useful drugs were developed from lead compounds discovered from plants [4]. For examples, many current chemotherapeutic drugs, including bleomycin, doxorubicin, mitomycin, vinblastine, vincristine, etoposide (VP16), topotecan, irinotecan, paclitaxel and combretastatins, are natural products or their derivatives [5]. Thus, pharmacologically active compounds from plants represent an important pool for new investigative drugs [6–10].

Chamaecyparis obtusa var. *formosana* Rehd. (Taiwan hinoki; Cupressaceae) is a type of timber which is highly available in Taiwan. We have previously investigated the chemical components of the heartwood of this plant and found various monoterpenes, sesquiterpenes, diterpenes and lignans [11–14]. Other than those phytochemicals, a novel skeleton compound, chamaecypanone C (Fig. 1), had been elucidated as a dimeric of monoterpene and norlignan with tricycle[5.2.2.$0^{2,6}$]undecane, also isolated from the heartwood of this plant [12]. Notably, this novel compound exhibited better growth inhibition properties with IC_{50} values ranging from 190 to 520 nM in three different human cancer cell lines, as compare to the clinically available anticancer drug VP16 [12]. However, the detailed molecular functions of this compound have not been dissected previously. In the present study, we investigated the mechanism of action of chamaecypanone C. We further determine the anticancer efficacy of this compound in various human cancer cells with multidrug resistant properties.

2. Materials and methods

2.1. Purification of Chamaecypanone C

The compound was isolated at the College of pharmacy, China Medical University (Taichung, Taiwan) with use of the method described by Chien et al. [12]. In brief, the air-dried slices of heartwood of *C. obtusa* var. *formosana* were extracted with acetone at room temperature. After evaporation of acetone, the extract was partitioned with an ethyl acetate–water mixture to give an ethyl acetate-soluble fraction and an aqueous phase. The ethyl acetate-soluble fraction was repeatedly chromatographed on silicon dioxide column and HPLC [Merck Lichrosorb Si 60, 100 × 10 mm i.d., ethyl acetate–dichloromethane (3:2)] to give chamaecypanone C. The chemical structure of chamaecypanone C was confirmed by ^{1}HNMR, ^{13}CNMR and EI-MS. The stock solution of chamaecypanone C was prepared in dimethyl sulfoxide (DMSO) and kept at −20 °C and diluted in PBS buffer to appropriate concentrations before every experiment.

2.2. Reagents

Colchicine, paclitaxel and vincristine were purchased from Sigma Chemical Co. (St. Louis, MO). Antibodies were obtained from following companies: α-tubulin (Sigma), Bcl2, Cdc2, Cdc25C, cyclin B1, Fas and horseradish peroxidase (HRP)-conjugated secondary antibody (Santa Cruz Biotechnology, Inc., Santa Cruz, CA), phosphospecific MPM-2 (Upstate Biotechnology, Lake Placid, NY), PARP (Severigen, Gaithersburg, MD), Fas-L (Oncogene Research Products, Darmstadt, Germany), FasL neutralizing monoclonal antibody 4A5 (MBL, Nagoya, Japan) and fluorescent isothiocyanate (FITC)-conjugated secondary antibody (Ancell Corporation, Bayport, MN). Recombinant human Fas/Fc chimera was purchased from R&D System (Minneapolis, MN). Medium and reagents of cell culture were acquired from Invitrogen (Carlsbad, CA). Microtubule-associated protein (MAP)-rich tubulin and biotin-labeled tubulin were from Cytoskeleton, Inc. (Denver, CO). [^{3}H]colchicine, [^{3}H]paclitaxel, [^{3}H]vinblastine and streptavidin-labeled poly(vinyl toluene) scintillation proximity assay (SPA) beads were purchased from Amersham Pharmacia Biotech (Piscataway, NJ). Other chemicals not specified were from Sigma or Merck (Darmstadt, Germany) with standard analytical or higher grade.

2.3. Cell cultures

Human oral epidermoid carcinoma KB (According to ATCC comments, the KB cell line was originally derived from an epidermal carcinoma of the mouth but has now been shown to have HeLa characteristics), nasopharyngeal carcinoma HONE-1, gastric carcinoma TSGH, hepatocellular carcinoma Hep3B and HepG2 and lung adenocarcinoma CL1-0 and CL1-5 cells were maintained in RPMI 1640 medium supplied with 5% fetal bovine serum. All the above cell lines were procured from American Type Culture Collection (ATCC, Rockville, MD) except CL1-0 and CL1-5 which were gift from Dr. Pan-chyr Yang in National Taiwan University Hospital, Taipei, Taiwan, ROC. The drug resistant cell lines, including KB-TAX50, KB-7D, HONE1-CPT30 were maintained in complete medium containing an additional 50 nM paclitaxel, 7 μM VP16 and 100 nM camptothecin, respectively. KB-TAX50 cells were generated by paclitaxel-driven selection and displayed overexpression of P-gp170/MDR [6,8–10]. KB-7D cells were generated by VP16-driven selection, which displayed down-regulation of Top II and overexpression of MRP [15,16]. HONE1-CPT30 cells have a mutation at topoisomerase I (E418K) resulting in camptothecin resistance [17]. All drug resistant cells were incubated in the drug-free medium for three days before harvesting for the growth inhibition assay.

2.4. Growth inhibition assay

Cells in logarithmic growth phase were cultured at a density of 10,000 cells/mL/well in a 24-well plate. The cells were exposed to various concentrations of the test drugs for three generation times. At the end of the incubation period, cells were fixed and stained with 50% ethanol containing 0.5% methylene blue for 30 min. The

plates were washed five times with water and allowed to air-dry. The resulting colored residue was dissolved in 1% *N*-lauroylsarcosine and optical density was read at 570 nm using a microplate reader. The IC_{50} value resulting from 50% inhibition of cell growth was calculated graphically as a comparison with control growth. Each point represents the average of at least three independent experiments run in triplicate.

2.5. Cell cycle analysis

Cell cycle progression was monitored using DNA flow cytometry. After drug treatment, cells were trypsinized, washed with PBS and fixed in 80% ethanol at −20 °C for 1 h. The fixed cells were stained with 50 μg/ml RNase and 50 μg/ml propidium iodide (PI) at room temperature in the dark for 20 min. The DNA content was determined by a fluorescence-activated cell sorting IV flow cytometer (BD Biosciences, Franklin Lakes, NJ). For each analysis, 10,000 cells were counted and the percentage of cells in each phase was calculated using ModFit LT software (Verity Software House, Topsham, ME).

2.6. Western blot analysis

Cells were initially seeded at a density of 1×10^6 in 100 mm^2 dishes. After treatment for the indicated time with various concentrations of test drug, adherent cells were washed twice with PBS, gently scraped from the dishes, centrifuged, lysed in ice-cold lysis buffer (50 mM Tris, pH 7.4, 0.8 M NaCl, 5 mM $MgCl_2$, 0.5% NP-40, 1 mM phenylmethylsulfonyl fluoride and proteinase inhibitor aprotinin, leupeptin and pepstatin 20 μg/ml each). Lysates were centrifuged at 12,000 × *g* for 15 min and the supernatants were collected and quantified. Equal amounts of lysate (on a protein basis) were then differentiated by SDS-PAGE, blotted on PVDF membranes, conjugated with various specific primary antibodies and then probed with appropriate secondary antibodies. The immunoreactive bands were detected by the ECL method and visualized on Kodak Bio-MAX MR film.

2.7. Microscopic assessment of the mitotic index

Cells were treated with various concentrations of Chamaecypanone C for the indicative times. For Giemsa staining, medium was aspirated, cells were washed with PBS and lysed with hypotonic solution (75 mM potassium chloride) for 15 min. Then cells were fixed with methanol:acetic acid (3:1) for 10 min followed by a 5% Giemsa stain for 5 min. Mitotic Index (MI = number of mitotic cells/total number of cells), was determined by counting at least 200 cells (including mitotic and non mitotic cells for each condition).

2.8. In vitro microtubule assembly assay

In brief, 0.24 mg microtubule-associated protein-rich tubulin was mixed with various concentrations of test compound and incubated at 37 °C in 120 μl reaction buffer (100 mM PIPES, pH 6.9, 1.5 mM $MgCl_2$, 1 mM GTP and 1% (v/v) DMSO). The increase in absorbance was measured at 350 nm in a PowerWave X Microplate Reader (BIO-TEK Instruments, Winooski, VT) at 37 °C and recorded every 30 s for 30 min.

2.9. In vivo microtubule assembly assay

Cells at a density of 1×10^6/100 mm^2 dishes were treated with indicated concentrations of test agents for the selected treatment duration. Then, cells were washed with PBS three times before adding lysis buffer containing 20 mM Tris-HCl, pH 6.8, 1 mM $MgCl_2$, 2 mM EGTA, 1 mM PMSF, 1 mM orthovanadate, 0.5% NP-40 and 20 μg/ml proteinase inhibitor aprotinin, leupeptin and pepstatin. Supernatants were collected after centrifugation at 15,000 × *g* for 10 min at 4 °C. This yielded soluble tubulin dimers in the supernatant and polymerized microtubules in the pellet. Equal amounts of the two fractions (on a protein basis) were partitioned by SDS-PAGE. Immunoblots were probed with α-tubulin monoclonal antibody and secondary HRP-conjugated antibody. The blots were developed using an Enhanced Chemiluminescence reagent kit (Perkin–Elmer Life and Analytical Sciences, Boston, MA) followed by development on Kodak Bio-MAX MR film (Rochester, NY).

2.10. Immunocytochemistry

Cells attached to coverslips were treated with chamaecypanone C for 24 h. Cells were fixed in methanol/acetone (1:1 v/v) at −20 °C for 1 h and then washed with PBST for 5 min. Nonspecific sites were blocked by incubating with 5% skim milk in PBST for 1 h. A mouse monoclonal antibody against α-tubulin was diluted 1:500 in blocking solution and incubated for 2 h. Cells were washed with PBST twice (10 min each) to remove excess antibody and then probed with FITC-conjugated secondary antibody (1:200) for 1 h at room temperature. The images of α-tubulin with FITC staining were captured with an Olympus BX50 fluorescence microscope (Dulles, VA).

2.11. Time-lapsed video microscopy

Cells were prepared for analysis of microtubule dynamics in living cells by using time-lapsed video microscope. This equipment composes an imaging system with a differential interference contrast (DIC) microscopy (Leica DM IRB). The images were acquired by a highly sensitive charge-coupled device (CCD) camera (ORCA ER, Hamamatsu Photonics K. K., Japan). Briefly, cells expressed the green fluorescent protein (GFP)-tubulin were placed on a temperature-controlled stage at 37 °C. Time lapse imaging of the tubulin dynamics after various concentration treatment of drug was recorded for proper period. For live cell imaging, a climate chamber was used to maintain cell viability and activity. The imaging system was controlled by Metamorph (Universal Imaging, Downingtown, PA).

2.12. Tubulin competition-binding scintillation proximity assay (SPA)

Briefly, [^{3}H]colchicine, or [^{3}H]vinblastine sulfate (final concentration, 0.08 μM, or 0.25 μM, respectively), were mixed with tested compound and special long chain biotin-labeled tubulin (0.5 μg for colchicine-binding assay and 1.0 μg for vinblastine binding assay) and then incubated in 100 μl reaction buffer (80 mM PIPES pH 6.8, 1 mM EGTA, 10% glycerol, 1 mM $MgCl_2$ and 1 mM GTP) for 2 h at 37 °C. Streptavidin-labeled poly(vinyl toluene) SPA beads (80 μg, or 200 μg for colchicine, or vinblastine binding assay, respectively) were then added to each reaction mixture.

2.13. Annexin-V/PI binding assay

Cells were treated with various concentration of Chamaecypanone C for the indicated times and the Annexin-V-FLUOS staining kit (Roche Diagnostics, Mannheim, Germany) was used according to manufacturer's instructions to evaluate Annexin-V/PI positivity. Control cells stained with Annexin-V or PI alone were used to compensate for flow-cytometric ananlysis (FACS-Vantage, BD Biosciences, San Jose, CA). Annexin-V- and

PI-double-negative cells were defined as live cells. Annexin-V-positive, PI-negative cells were defined as early apoptotic cells and Annexin-V- and PI-double-positive cells were defined as late-arising apoptotic cells.

2.14. Determination of caspases activity

The activity of caspase 3, 8, 9 on Chamaecypanone C-treated cells were determined by using Caspase Fluorometric Assay Kits (R&D Systems Inc., Minneapolis, MN) or the CaspACE Assay System Fluorometric (Promega Corporation, Madison, WI) for the cleavage of respective specific fluorogenic peptide substrate according to the instruction of the manufacturer. Briefly, 3×10^6 cells were collected, lysed in a lysis buffer and clarified by centrifugation. Equal amounts of the extract supernatants were incubated with 50 μM of fluorescent substrate (Ac-DEVD-AMC, caspase 3 substrate; IETD-AFC, caspase 8 substrate; LEHD-AFC, caspase 9 substrate). After 1 h of incubation at 37 °C, fluorescence of the cleaved substrate was determined using the Victor 1420 Multilable Counter (Wallac, Turku, Finland) and caspase activity was calculated by subtracting the value obtained in the untreated sample.

Table 1
Growth inhibition of Chamaecypanone C against various human cancer cell lines.

Cell lines	Origin	IC_{50} (nM)[a]
KB[b]	Oral epidermoid carcinoma	220 ± 80
HONE1	Nasopharyngeal carcinoma	240 ± 80
TSGH	Gastric carcinoma	520 ± 110
HepG2	Hepatocellular carcinoma	840 ± 150
Hep3B	Hepatocellular carcinoma	780 ± 120
CL1-0	Lung adenocarcinoma	380 ± 70
CL1-5	Lung adenocarcinoma	290 ± 60

[a] Each value represented the mean ± S.D. of three independent experiments.
[b] According to *ATCC* comments, the KB cell line was originally derived from an epidermal carcinoma of the mouth but has now been shown to have HeLa characteristics.

2.15. Caspases inhibitory assay

In the caspase inhibitory experiments, the Z-DEVD-fmk, Z-IETD-fmk, Z-LEHD-fmk of cell-permeable and specific irreversible inhibitors of caspase 3, 8, 9, respectively (Calbiochem, La Jolla, CA), were added to the medium 1 h prior to Chamaecypanone C administration. Cell survival was determined by the methylene

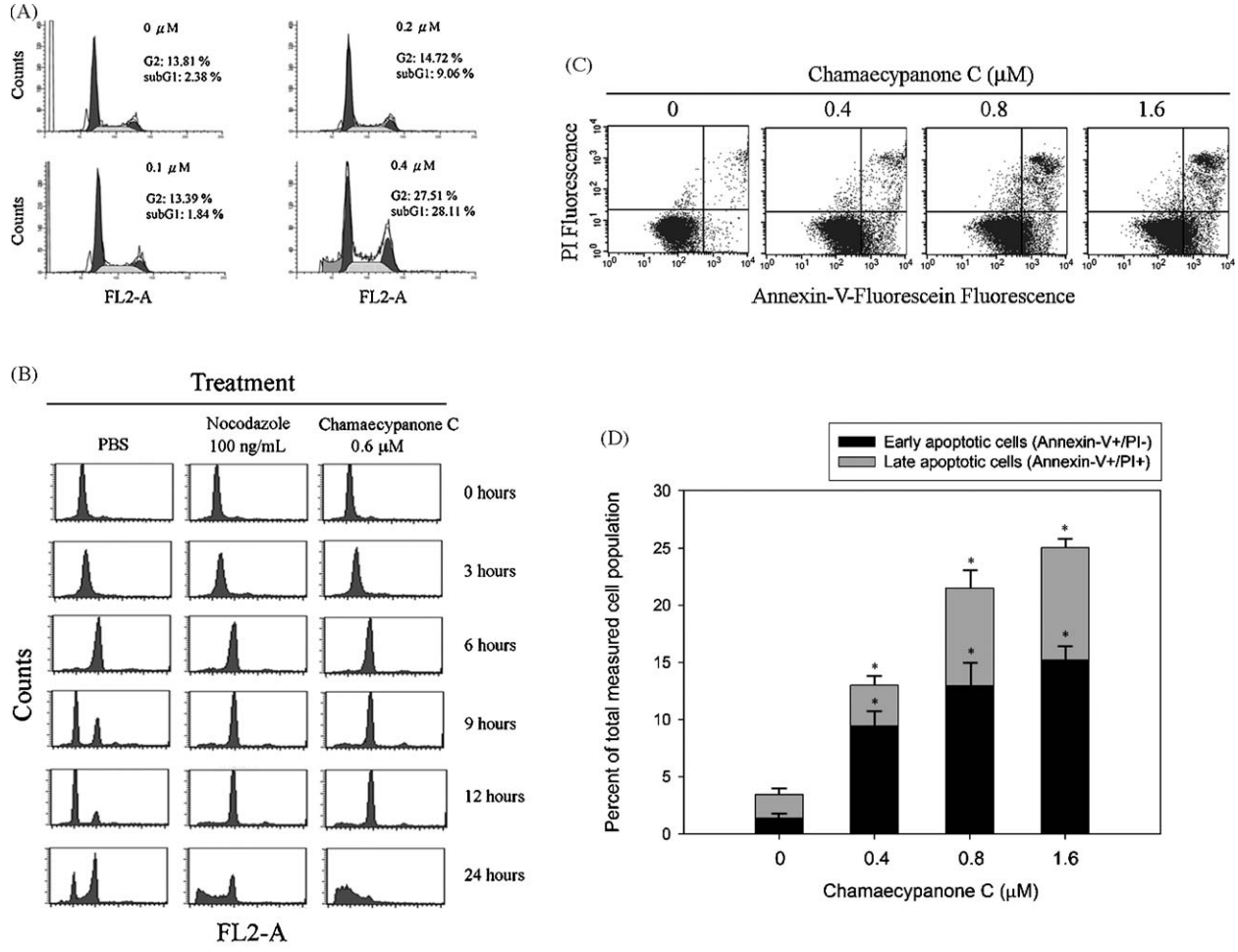

Fig. 2. Chamaecypanone C induces G2/M phase arrest before apoptotic cell death occurs. (A) The dose effect of Chamaecypanone C on cell cycle distribution in KB cells. Cells were treated with various concentrations of Chamaecypanone C for 24 h and analyzed for PI-stained DNA content by flow cytometry. (B) The time effect of Chamaecypanone C on cell cycle distribution in double thymidine synchronized cells. Cells were synchronized at the G_1/S transition by a double thymidine treatment for 17 h, then were washed, shifted to complete medium and treated with test compounds. Cells were collected at the indicated time points after release from the second thymidine block. Cells were fixed and stained with PI and the DNA content was analyzed by flow cytometry. (C) Chamaecypanone C-induced cell underwent apoptosis as demonstrated by Annexin-V positivity. Cell were treated with various concentrations of Chamaecypanone C for 24 h then incubated with Annexin-V and PI and subjected to flow cytometric analysis. Quantitative result of Annexin-V/PI positivity has been shown in (D). The data represent the mean ± S.D. of three independent experiments. Black bars: early apoptotic cells (Annexin-V+/PI−); gray bars: late apoptotic cell (Annexin-V+/PI+). Student's *t*-test was calculated to compare the mean of each group with that of the control group. *, A p value < 0.05 was considered statistically significant.

blue dye assay as describe in "growth inhibition assay" to evaluate the effects of the test compound on cell growth.

2.16. FasL neutralization assay

FasL-dependent cell death was evaluated by a neutralization assay. 2 μg/mL of FasL neutralizing monoclonal antibody 4A5 (MBL, Nagoya, Japan) and recombinant human Fas/Fc chimera (R&D System, Minneapolis, MN) were added to the cell culture 1 h prior to Chamaecypanone C administration. After 16 h, the percentage of apoptotic cells was assessed by Annexin-V/PI binding assay to evaluate the role of FasL involvement in the mechanism.

2.17. Statistical analysis

All assays were carried out in triplicate. Data were expressed as means with standard deviations. Student's *t*-test was calculated to compare the mean of each group with that of the control group. A p value < 0.05 was considered statistically significant.

3. Results

3.1. Chamaecypanone C induced growth inhibition in human cancer cell lines

Initial experiments were conducted for evaluation of growth inhibition by Chamaecypanone C against various types of human cancers *in vitro*. The results showed that Chamaecypanone C inhibited the growth of several human cancer cell lines including KB, which was originally derived from an epidermal carcinoma of the mouth but has now been shown to have HeLa characteristics, HONE-1 (nasopharyngeal carcinoma), TSGH (gastric carcinoma), CL1-0 and CL1-5 (lung adenocarcinoma) cells, with IC_{50} values ranging from 200–500 nM (Table 1). However, Chamaecypanone C possessed less potent against two hepatocellular carcinoma cell lines, HepG2 and Hep3B, with IC_{50} values around 800 nM (Table 1).

3.2. Chamaecypanone C induced G_2–M phase arrest and subsequent apoptotic cell death

The effect of Chamaecypanone C on cell cycle progression was examined by flow cytometry. KB cells were incubated with various concentrations of Chamaecypanone C for 24 h. In asynchronous-culturing conditions, the flow cytometeric analysis clearly revealed that Chamaecypanone C caused an increase in the number of KB cells in G_2–M phase (Fig. 2A). We further synchronized KB cells at the G_1–S phase by a double thymidine treatment and then cells were treated with either PBS, 100 ng/ml of nocodazole, or 0.6 μM of Chamaecypanone C for the indicative times. As shown in Fig. 2B, nocodazole- and Chamaecypanone C-treated cells showed delayed-transition into the G_1 phase from the G_2–M phase. Furthermore, a typical apoptosis-related hypodiploid DNA content peak (sub-G_1) was detected in the nocodazole- and Chamaecypanone C-treated cells after 24 h (Fig. 2B). For further assessing the apoptotic population of Chamaecypanone C-treated cells, we performed Annexin V-PI binding assay. As shown in Fig. 2C, Chamaecypanone C induced apoptosis in cells in a concentration-dependent mannar. Taken together, these results indicate that Chamaecypanone C inhibited cancer cell growth by arresting cells in the G_2–M phases and subsequent activated the apoptotic signaling pathway.

3.3. Chamaecypanone C-induced changes in the expression and phosphorylation of G_2–M regulators

We further investigated the association between Chamaecypanone C-induced G_2–M phase arrest and alteration in the expression of G_2–M regulatory proteins. Western blot analysis revealed that Chamaecypanone C induced the expression of cyclin B1 in cells in a concentration-dependent manner (Fig. 3A). In addition, up-shifting of the Cdc25 band was shown in the Chamaecypanone C-treated cells. These results indicated that Chamaecypanone C induced Cdc25C phosphorylation in cells. On the other hand, Chamaecypanone C-induced the de-pohosphorylation of Cdc2 in a concentration-dependent manner (Fig. 3A).

We further examined the status of phosphorylated polypeptides found only in mitotic cells using MPM-2 antibody. The levels of MPM-2 phosphoepitopes were increased in cells treated with Chamaecypanone C for 24 h, as shown by western blotting (Fig. 3B). To quantities the amount of cells under mitotic arrest, cells were stained with Giemsa dye and the percentages of mitotic cells were analyzed. As shown in Fig. 3C, Chamaecypanone C significantly increased the mitotic index of KB cells in concentration-dependent manner. This result indicated that Chamaecypanone C induces

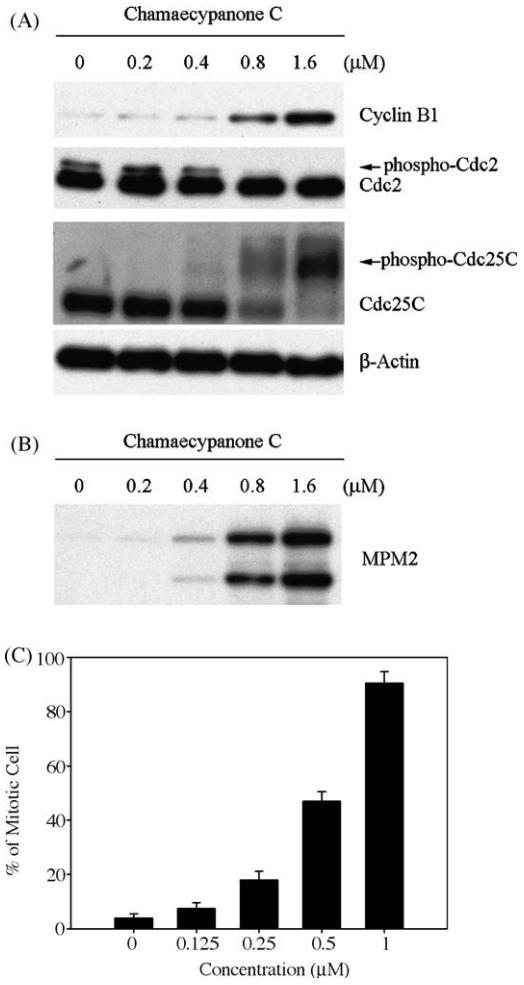

Fig. 3. Chamaecypanone C-induced change in G_2–M regulators coincides with mitotic arrest occurs in KB cells. (A) Change in expressed and phosphorylated status of G_2–M regulators after Chamaecypanone C treatment. Cells were harvested after Chamaecypanone C treated for 24 h and cell extract was prepared and loaded on SDS-PAGE. After eletrophoresis, proteins were transferred to blots and probed with cycin B1, Cdc2, Cdc25C, as well as internal control, β-actin antibodies. (B) Evaluation the appearance of mitotic marker, MPM-2 phosphoepitopes, in Chamaecypanone C-treated cells. Cells were harvested after Chamaecypanone C treated for 24 h and cell extract was prepared and loaded on SDS-PAGE. After eletrophoresis, proteins were transferred to blots and probed with MPM-2 antibody. (C) Quantitative assessment of mitotic arrest by Chamaecypanone C. Cells were treated with different concentrations of Chamaecypanone C for 24 h and then stained with Giemsa dye. The mitotic cells were counted for at least 200 cells. Each point represents the mean ± S.D. of three independent experiments.

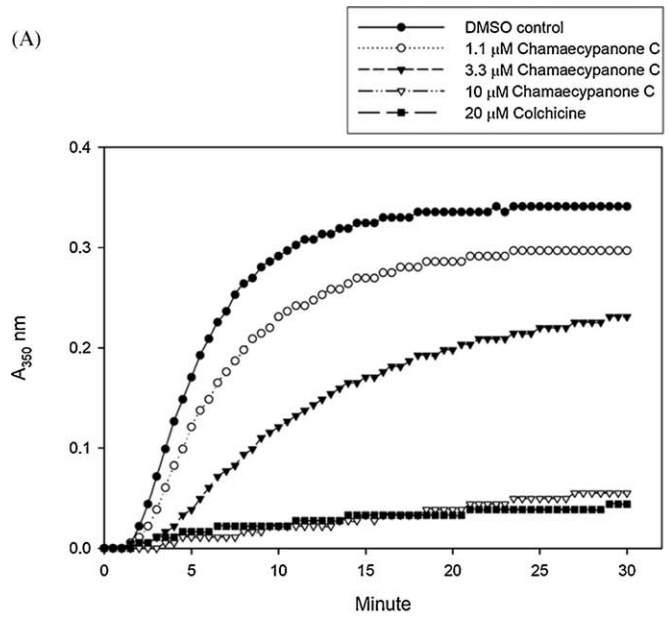

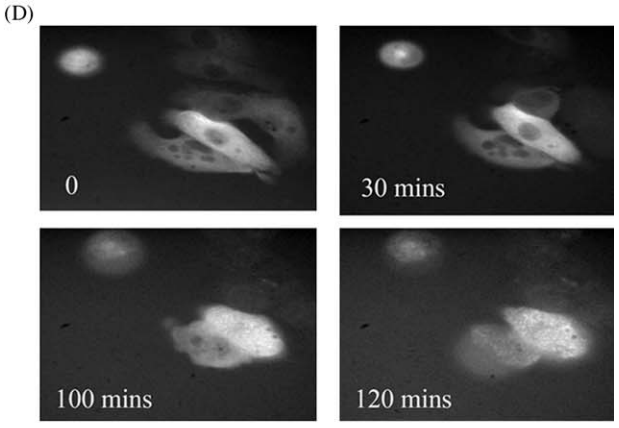

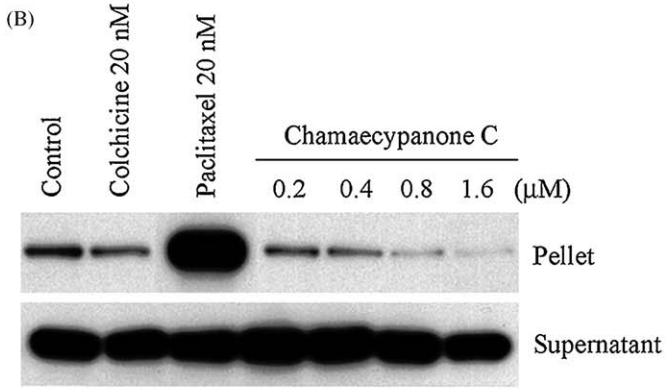

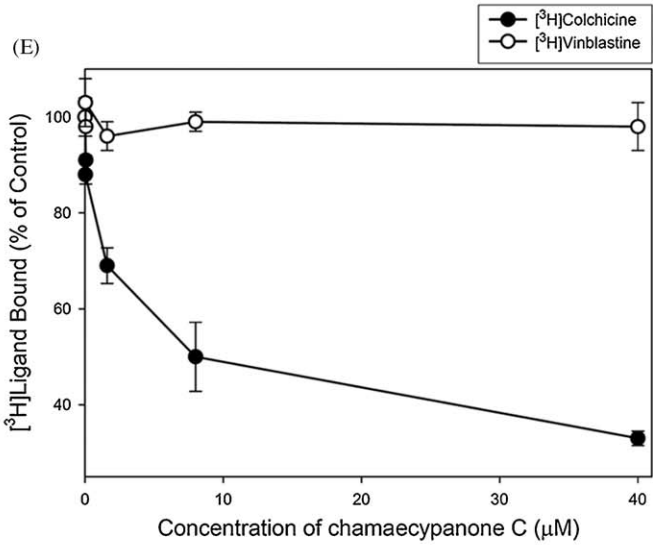

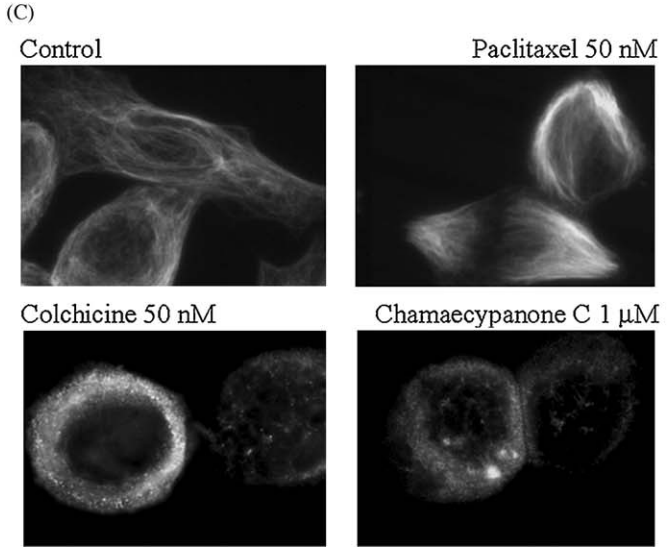

Fig. 4. Chamaecypanone C inhibits microtubule assembly through binds to the colchicine-binding site of tubulin. (A) Effect of Chamaecypanone C on tubulin polymerization *in vitro*. MAP rich tubulins were incubated at 37 °C in the absence or presence of drug. Absorbance at 350 nM was measured every 30 s for 30 min and is presented as the increased polymerized microtubule. (●) DMSO control; (○) 1.1 μM Chamaecypanone C; (▼) 3.3 μM Chamaecypanone C; (▽) 10 μM Chamaecypanone C; (■) 20 μM colchicine. (B) Chamaecypanone C inhibits microtubule assembly *in vivo*. Cells were treated with test drugs or with the same volume of DMSO in PBS as control. After 24 h incubation, cells were lysed in lysis buffer. Cell lysates were centrifuged to separate polymerized microtubules (pellet) form tubulin dimers (supernantant) as described in Section 2. After gel electrophoresis and transfer to nitrocellulose membrane, α-tubulin was visualized by Western blotting. (C) Effect of Chamaecypanone C on the organizations of cellular

changes in the expression and phosphorylation of G_2–M regulators such as Cdc25C, Cdc2 and MPM2. Chamaecypanone C also induces mitotic arrest in KB cells.

3.4. Chamaecypanone C binds to the colchicine-binding site of tubulin and inhibits microtubule assembly

Since Chamaecypanone C induced mitotic arrest, we wondered whether this compound interferes with microtubule dynamics. To determine the effect of Chamaecypanone C on microtubule assembly *in vitro*, we incubated purified, unpolymerized, microtubule-associated protein-rich tubulin with various concentration of Chamaecypanone C and level of tubulin polymerization was measured. In the DMSO control (w/o drug), rapid increases in tubulin polymerization within 10 min of incubation was shown (Fig. 4A). Colchicine was used as an inhibition positive-control. Here, colchicine successfully inhibited the polymerization of tubulin as expect (Fig. 4A). In the presence of Chamaecypanone C, tubulin polymerization was also inhibited in a concentration-dependent manner (Fig. 4A). Next, we studied the effect of Chamaecypanone C on the dynamics of microtubule assembly at the cellular level after 24 h of treatment. Paclitaxel was used as a polymerization positive-control. As shown in Fig. 4B, the polymerization of tubulin was increased in paclitaxel-treated cells compared to the control cells. Cells treated with vincristine or colchicine (tubulin de-stabilizers) showed a decreased amount of the tubulin polymers as expected. In comparison, Chamaecypanone C also inhibits tubulin polymerization in a concentration-dependent manner (Fig. 4B).

We further examined the effect of Chamaecypanone C on cellular microtubule networks by using immunofluorescence techniques. In drug-free situations, the microtubule network exhibited normal arrangement and organization in KB cells (Fig. 4C, top left). However, 50 nM of a tubulin de-stabilizer, colchicine, significantly induced cellular microtubule depolymerization with short microtubules in the cytoplasm after 24 h (Fig. 4C, bottom left). In contrast, 50 nM of a tubulin stabilizer, paclitaxel, promoted microtubule polymerization with an increase in the density of cellular microtubules and it also promoted the formation of long thick microtubule bundles (Fig. 4C, top right). It is interesting to note that Chamaecypanone C treatment induces similar changes to the microtubule networks in cells, as compared to the colchicines treatment. In Chamaecypanone C-treated cells, loss of intact microtubule networks throughout the cytoplasm was clearly shown (Fig. 4C, bottom right). Microtubule dynamics in cells treated with Chamaecypanone C were further analyzed by the time-lapsed video microscopy. Real-time imaging of the dynamics of microtubule in cells treated with 12 μM of Chamaecypanone C was recorded for 2 h. As shown in Fig. 4D, microtubules starting to disrupt in cells treated Chamaecypanone C 100 min post-treatment (Fig. 4D, bottom left). Furthermore, a diffuse pattern which indicates complete disruption of the microtubule networks was shown in cells treated with Chamaecypanone C for 120 min (Fig. 4D, bottom right).

Since Chamaecypanone C inhibits microtubule assembly in a way similar to colchicine and vinblastine, we performed the competition-binding SPA assay to determine whether Chamaecypanone C binds to the same intracellular target as those compounds. Experimental results revealed that Chamaecypanone C did not reduce the specific SPA counts stimulated by conjugating the biotin-labeled tubulin with [^{3}H]vinblastine, but it strongly competed with [^{3}H]colchicine-binding to tubulin (Fig. 4E). Taken together, our result indicated that Chamaecypanone C inhibits microtubule assembly through binding to the colchicine-binding site of tubulin.

3.5. Chamaecypanone C induces apoptotic cell death through caspase 8-Fas/FasL dependent pathway

Since Chamaecypanone C induced G_2–M phase arrest and subsequent activation of the apoptosis in KB cells, we therefore investigated the effects of Chamaecypanone C on caspases. Of many caspases involve in the process of apoptosis, we firstly examined the effect of Chamaecypanone C on caspase 3, which is activated by a number of apoptotic signals. As shown in Fig. 5A, incubation of KB cells with Chamaecypanone C for 24 h resulted in the activation of caspase 3 in a concentration-dependent manner. Activation of caspase 3 during Chamaecypanone C-induced apoptosis was also confirmed by examining PARP. PARP is an endogenous substrate for caspase 3 and it is an early marker of apoptosis. Western blot analysis revealed that Chamaecypanone C induced the cleavage of PARP (116 kDa) into an 85 kDa C-terminal fragment in cells in a concentration-dependent manner (Fig. 5B).

To understand the mechanism by which caspase 3 is activated by Chamaecypanone C, we further investigated the effect of this compound on the activity of caspase 8 and 9, upstream activators of caspase 3. Chamaecypanone C induces the activation of caspase 8 and 9 in cells (Data not shown). To further elucidate the role of caspase 8 and 9 in Chamaecypanone C-induced cytotoxicity, cells pre-treated with membrane-permeable irreversible inhibitor of caspase 3 (Ac-DEVD-AMC), 8 (IETD-AFC), or 9 (LEHD-AFC) and incubated with various concentrations of Chamaecypanone C. Cell viability assay revealed that Chamaecypanone C induced growth inhibition was significantly reduced in the cells pre-treated with caspase 8-specific inhibitor (IETD-AFC) and caspase 3 inhibitor (Ac-DEVD-AMC) (Fig. 5C). In contrast, cells pre-treated with the caspase 9 specific inhibitor (LEHD-AFC) did not prevent Chamaecypanone C induced cell death (Fig. 5C). These results indicated that Chamaecypanone C induces apoptosis through activation of caspase 8 and downstream caspase 3.

Since caspase 8 is one of the most apical caspases in Fas/FasL mediated apoptosis, Fas/FasL expression in Chamaecypanone C-treated cells was assessed by western blotting. As shown in Fig. 5D, FasL expression was induced significantly by Chamaecypanone C in concentration-dependent manner in KB cells. However, the expression of Fas protein was not modulated by Chamaecypanone C.

In order to determine whether FasL upregulation would play a role in Chamaecypanone C induced apoptosis of KB cells, we used an anti-FasL neutralizing monoclonal antibody 4A5 and a recombinant Fas/Fc chimera that have been shown to inhibit the induced apoptosis of the FasL. Two μg/mL of FasL neutralizing monoclonal antibody 4A5 and recombinant human Fas/Fc chimera were added to the cell culture 1 h prior to Chamaecypanone C administration. After 16 h, the percentage of apoptotic cells was assessed by Annexin-V/PI binding assay. Our result demonstrated that both of neutralizing antibody 4A5 and Fas/Fc chimera were able to block 50 and 40% of the FasL-induced apoptosis in KB cells, respectively (Fig. 5E and F). This result indicated that Chamaecypanone C-induced apoptosis of KB cells is mediated at least partly through the Fas/FasL pathway.

microtubule network. Cells were treated with test drug for 24 h. After incubation, cells were harvested and fixed with fix solution. Fixed cells were reacted with monoclonal anti-α-tubulin antibody at room temperature for 2 h. After reacted with FITC-conjugated secondary antibody, the cellular microtubules were observed by OLYMPUS-BX50 fluorescence microscope. (D) Time-lapse sequence of microtubule in living cells. Cells expressed the GFP-tubulin were prepared for analysis of microtubule dynamics in living cells by using time-lapsed video microscope. Time-lapsed imaging of the microtubule dynamics after 12 μM Chamaecypanone C treatment was recorded for up to 2 h. (E) Chamaecypanone C binds to colchicine-binding site of tubulin. Tubulin was incubated with the radiolabeled ligand at 37 °C and the amount of radioligand bound was determined by using scintillation proximity assay beads. [^{3}H]colchicine and [^{3}H]vinblastine competition-binding curves. Each data point, the mean ± S.D.

3.6. Chamaecypanone C is cytotoxic toward multi-drug resistant cancer cell line

One major mechanism of acquired drug resistance is the overexpression of efflux pumps, namely, P-gp170/MDR and MRP. Cell lines selected for expression of drug efflux pumps by long-term drug exposure were used to exam the anti-tumoral activity of Chamaecypanone C. As shown in Table 2, despite the high level of expression of drug resistant efflux proteins (P-gp170/MDR or MRP) in Hela subline KB-TAX50 and KB-7D cells, Chamaecypanone C showed a similar cytotoxic efficacy between parental and resistant sublines. In addition, Chamaecypanone C also displayed potent anti-proliferative activity against the topoisomerase I-mutanted HONE1-CPT30 cells (Table 2).

4. Discussion

In the past three decades, microtubules continue to be one of the most successful cancer chemotherapeutic targets [18–22]. Taxenes and *Vinca* alkaloids are well-characterized anti-mitotic

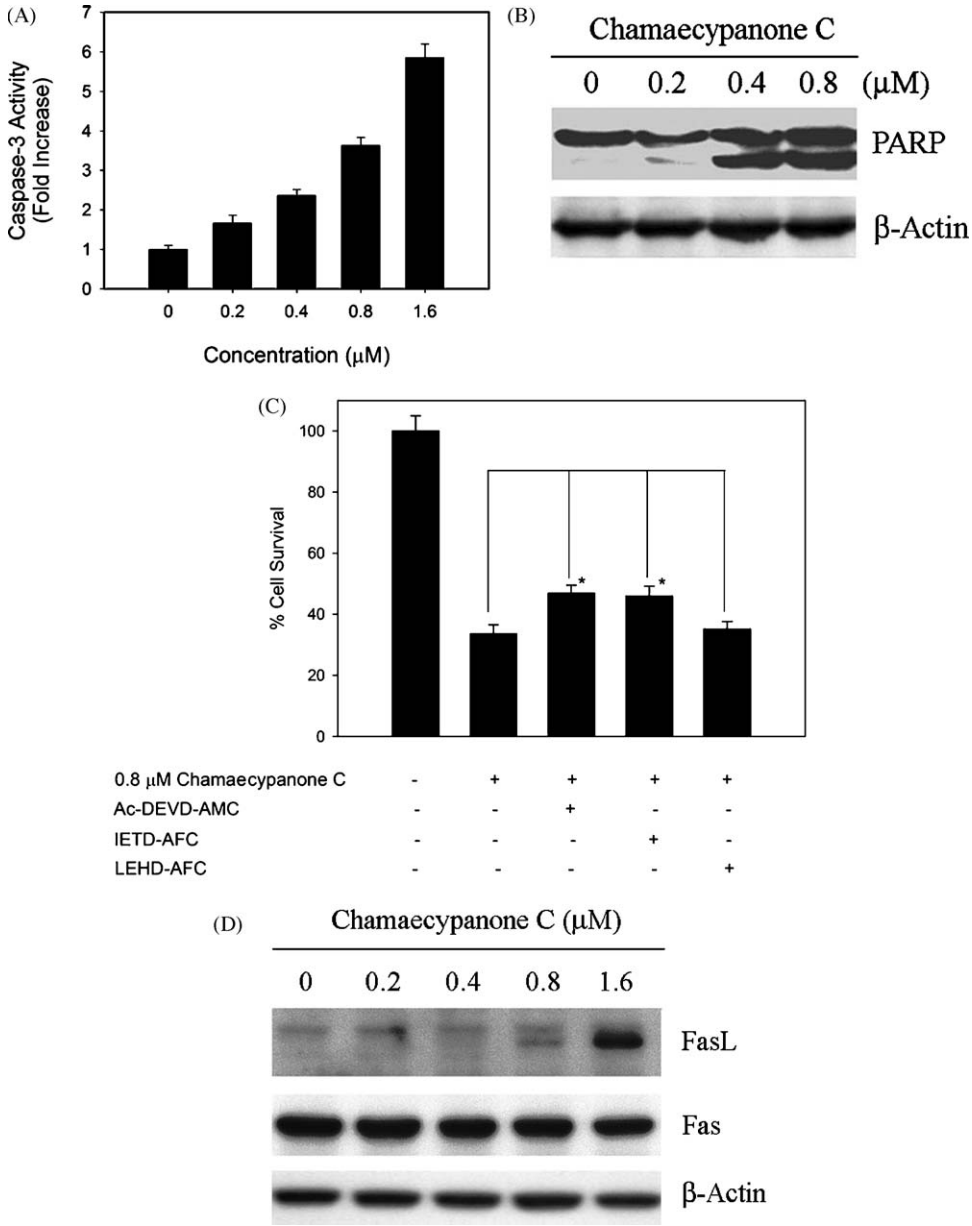

Fig. 5. Chamaecypanone C induced apoptotic cell death mainly through the caspase 8/Fas–FasL cascade. (A) Dose dependent increase in caspase 3 activity in KB cells after Chamaecypanone C treatment. Cells were treated with various concentrations of test drug for 24 h and analyzed caspase 3 activity using the fluorogenic tetrapeptide Ac-DEVD-AMC cleavage assay. Each point represents the mean ± S.D. (B) Chamaecypanone C induced PARP cleavage. Cells were treated with various concentrations of test drug for 24 h and the cleavage of PARP was examined by Western blot analysis. (C) Chamaecypanone C-induced cell death is reduced with caspase inhibitors. Cells were pretreated with 100 μM of the cell-permeable and specific irreversible caspase inhibitors (Z-DEVD-fmk, caspase 3 inhibitor; Z-IETD-fmk, caspase 8 inhibitor; Z-LEHD-fmk, caspase 9 inhibitor) for 1 h, then treated with 0.8 μM Chamaecypanone C for 24 h. The cell survival was determined by the methylene blue dye assay. Values are the means of triplicate analysis. Error bars show the standard deviations. *, significantly different from the Chamaecypanone C alone group at $p < 0.05$ with Student's t test. (D) Effect of Chamaecypanone C on Fas and FasL expression on KB cells. Cells were treated with various concentrations of Chamaecypanone C for 24 h. Cellular extracts were prepared and analyzed by SDS-PAGE and Western blot analysis. (E) Neutralization of FasL reduces Chamaecypanone C-induced apoptosis. KB cells were treated with 2 μg/mL of FasL neutralizing monoclonal antibody 4A5 and recombinant human Fas/Fc chimera 1 h prior to 0.8 μM of Chamaecypanone C administration. After 16 h, the percentage of apoptotic cells was assessed by Annexin-V/PI binding assay. Quantitative result of Annexin-V/PI positivity in FasL neutralization assay has been shown in (F). The data represent the mean ± S.D. of three independent experiments. Black bars: early apoptotic cells (Annexin-V+/PI−); gray bars: late apoptotic cell (Annexin-V+/PI+). *, A p value < 0.05 was considered statistically significant between control group and Chamaecypanone C treatment; #, a p value < 0.05 was considered statistically significant between Chamaecypanone C alone and combined with Fas/FasL antagonists treatment.

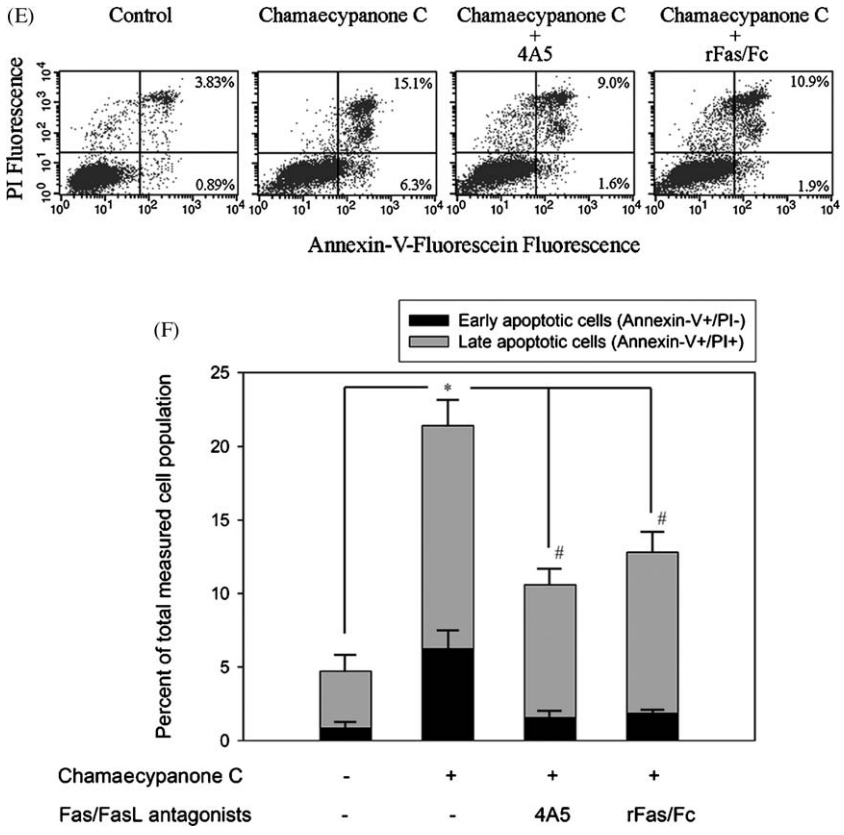

Fig. 5. (*Continued*).

Table 2
Growth inhibition of Chamaecypanone C against drug-resistant cell lines.

Cell lines[a]	Resistant type	IC_{50} [b]				
		Chamaecypanone C (nM)	Vincristine (nM)	Paclitaxel (nM)	VP16 (μM)	Camptothecin (nM)
KB	(Parental)	220 ± 80	0.4 ± 0.2	3.3 ± 1.2	1.1 ± 0.2	43.3 ± 2.4
KB-TAX50	P-gp170/MDR	241 ± 50	1.8 ± 0.5	273 ± 15	3.5 ± 0.3	55.7 ± 5.9
KB-7D	MRP ↑	144 ± 50	1.2 ± 0.4	7.9 ± 0.5	54 ± 3.5	133 ± 16
HONE1	(Parental)	280 ± 80	1.4 ± 0.3	2.7 ± 0.4	0.5 ± 0.1	27 ± 5.1
HONE1-CPT30	Top 1 mutant	230 ± 70	1.6 ± 0.2	2.8 ± 0.6	0.4 ± 0.1	355 ± 30

[a] All resistant cell lines are maintained in drug-free medium for 3 days before seeding for growth inhibition assay.
[b] Each value represented the mean ± S.D. of three independent experiments.

compounds which are widely used in clinical situations. However, the development of multidrug resistance limited the potency of these anti-mitotic compounds [23]. Therefore, there has been a great interest in identifying novel microtubule inhibitors that can overcome various modes of resistance and exhibits improved pharmacology profiles [6,8,10,24–28]. In this study, a novel anti-mitotic compound, Chamaecypanone C, was isolated from the heartwood of *Chamaecyparis obtusa* var. *formosana* and we have shown for the first time that this compound carries anticancer properties. Furthermore, we described the cellular and molecular events underlying the growth inhibitory effect of this compound in human cancer cells.

Drug resistance is a common problem in the management of neoplastic disease and the effectiveness of many clinically useful drugs is limited by the fact that they are substrates for the efflux pumps P-gp170/MDR and MRP [6,23,29]. In this study, unlike traditional chemotherapeutic compounds such as vincristine, paclitaxel, VP16 and camptothecin, Chamaecypanone C was shown to be effective against drug resistant cells despite P-gp170/MDR or MRP status. Moreover, Chamaecypanone C was also effective against camptothecin-resistant cancer cell lines. Taken together, our results suggested that Chamaecypanone C is not a substrate of these drug resistance-related efflux pumps and that it can be used to target cancer cells that are resistant to traditional chemotherapeutic compounds.

In the current study, Chamaecypanone C arrests the growth of KB cancer cells at the G_2–M phase (Fig. 2). It is well-demonstrated that different classes of cyclins and their cyclin-dependent kinases control cell cycle progression. In eukaryotic cells, cyclin B and Cdc2 kinase regulate the onset of mitotic phase (M phase). Activation of Cdc2 kinase at G_2–M transition requires accumulation of cyclin B and dephosphorylation of Cdc2 [30]. The conversion of Cdc2 from inactive to active form is processed by the specific phosphatase, Cdc25C [31,32]. Phosphorylation of Cdc25C self-activates its phosphatase function and subsequent activates Cdc2/cyclin B1 kinase to facilitate cell cycle entry into the M phase [33]. In this study, we demonstrated that cells treated with Chamaecypanone C leads to the accumulation of cyclin B1 and subsequent initiates a phosphoylation cascade, resulting in the engagement of active Cdc2 kinase and phosphorylation of Cdc25C (Fig. 3A). Furthermore, changes in Cdc2 and Cdc25C status coincide with increases in mitotic indices and the appearance of mitosis-related phosphoepitopes MPM-2 (Fig. 3B and

C) [34]. These results gave first indication that Chamaecypanone C inhibits cancer cell growth, possibly through interference with mitosis.

Successful completion of the mitosis requires dynamic changes of the microtubule networks. In cells, microtubule filaments rapidly alternate between phases of growth and shrinkage (dynamic instability) during cell cycle. Since microtubules play crucial roles in the regulation of the mitotic apparatus, disruption of microtubules can induce cell cycle arrest in M phase, the formation of abnormal mitotic spindles and final triggering of signals for apoptosis. Our data clearly demonstrated that Chamaecypanone C depolymerizes microtubules by binding to the colchicine-binding site of tubulin (Fig. 4). Currently, the *vinca* domain, the taxane site and colchicine site are three well documented anti-mitotic drug binding sites of the β-tubulin [35]. The colchicine site is located at the intra-dimer interface between β-tubulin and α-tubulin subunit [36]. Compounds binding to the colchicine-binding site typically induce microtubule depolymerization. For examples, a South African willow *Combretum caffrum* extracted compound, combretastatin A-4 (CA-4), inhibits microtubule assembly through binding to colchicine-binding site of tubulin and it exhibits potent anticancer activity by inhibiting cell cycle progression at mitosis and triggering apoptosis [37]. In addition to CA-4, podophyllotoxin, halichondrin B, curacin A, 2-methoxyestradiol, nacodazole, sulfonamides, etc., has similar mechanism of action in regulation of microtubules [19,38]. Thus, development of anti-mitotic compounds which are able to bind to the "colchicine site" has recently gained intensive interest. Here, we demonstrated that Chamaecypanone C, with a dimeric of monoterpene–norlignan–tricycle[5.2.2.$0^{2.6}$] undecane structure, exhibits anti-mitotic properties.

It is widely accepted that microtubule-interfering agents induce apoptosis by initiating cell cycle arrest [39]. Besides microtubules destabilization and cell cycle inhibition, our study also demonstrated that Chamaecypanone C provokes apoptosis in cancer cells, as indicated by an increase in the amount of sub-G_1 population in the drug-treated cells. Results from the annexin V assay, caspase 3 activity assay and western blot analysis further supported the above statement (Fig. 2 and 5A and B). There are two important apoptosis pathways which caspases play important role: (1) "death receptors" related extrinsic pathway and (2) mitochondria related intrinsic pathway [40]. Several evidences indicated that Bcl-2 is a guardian of microtubule integrity and it also plays important role in the intrinsic apoptosis [41]. Microtubule inhibitors such as vincristine, vinblastine, colchicine, paclitaxel and doxetaxel induce growth arrest, subsequent phosphorylation and inactivation of Bcl-2 and finally apoptotic cell death through caspase 9-dependent pathway [8,10,42–46]. Surprisingly, unlike traditional microtubule inhibitors which we have mentioned above, Bcl-2 hyperphosphorylation and mitochondria damage were not observed in Chamaecypanone C-treated cancer cells (Data not shown). In addition, addition of caspase 9 inhibitor could not rescue Chamaecypanone C-induced cell death *in vitro* (Fig. 5C). These results indicated that Chamaecypanone C induced apoptosis through caspase 9 independent mechanism.

Fas is a death domain-containing member of the tumor necrosis factor receptor family and its ligand, FasL, have been predominantly studied with respect to their capability to induce caspase 8 dependent cell death. Our current study reveals that the induction of apoptosis was preceded by increased expression of FasL (Fig. 5D), which was followed by subsequent activation of caspase 8 and 3. In the presence of specific caspase 8 and 3 inhibitors as well as FasL neutralizing antibody 4A5 and recombinant human Fas/Fc chimera, Chamaecypanone C-induced cell death was significantly inhibited, as compared to the control without any treatment (Fig. 5C, E, and F). These results indicated that Chamaecypanone C-induced apoptosis of KB cells is mediated at least in part by interfering with the Fas/FasL-signaling cascade. It is well-documented that activation of the Fas/FasL complex triggers rapid induction of apoptosis in cells [47–50]. Interestingly, Torgler et al. indicated that activation of cyclin B1 appears to be mediated through the formation of cyclin B1/Cdc2 complex. The author further demonstrated that overexpression of cyclin B1 enhances FasL promoter activity. Thus, cyclin B1 has been implicated in Fas/FasL-dependent cell death [51]. Since Chamaecypanone C induced inappropriate accumulation of cyclin B1 and activation of Cdc2 kinase in cells (Fig. 3A), therefore Chamaecypanone C may indirectly activates Fas/FasL signaling pathway through interference with the cell cycle.

Since those caspase inhibitors and Fas/FasL antagonists only possess partial effect in reversing Chamaecypanone C-induced apoptosis (Fig. 5C, E and F), there is not doubt that other factors/molecules may also involve in this death mechanism, which might account for the observed inconsistency of the effective dosage between FasL, caspase 3 and PARP expression in Chamaecypanone C-treated cells (Fig. 5A, B and D).

In conclusion, we demonstrate for the first time that a novel anti-mitotic compound Chamaecypanone C, with structure of a dimeric of monoterpene and norlignan with tricycle[5.2.2.$0^{2.6}$]undecane, exhibits anticancer properties. At the molecular level, this compound prevents microtubule assembly through binding to the colchicine-binding site of tubulin. Importantly, unlike other traditional anti-mitotic compounds, Chamaecypanone C induces apoptotic cell death through caspase 8 and Fas/FasL-dependent pathway. In addition, Chamaecypanone C is less subjective to the P-gp170/MDR and MRP related drug resistance. These findings indicate Chamaecypanone C is a promising new tubuliln-binding compound with potential for management of various malignancies, particularly for patients with demonstrated drug resistance. The unique structure and anticancer activity of Chamaecypanone C make it an interesting compound for further development.

Acknowledgements

This work was supported in part by grants from National Health Research Institutes, Taipei, Taiwan (NHRI intramural grant CA-098-PP-02), the National Science Council, Taipei, Taiwan (NSC98-2323-B-400-004), and China Medical University, Taichung, Taiwan (CMU98-CT-01).

References

[1] Lee S, Schmitt CA. Chemotherapy response and resistance. Curr Opin Genet Dev 2003;13:90–6.
[2] Kartner N, Riordan JR, Ling V. Cell surface P-glycoprotein associated with multidrug resistance in mammalian cell lines. Science 1983;221:1285–8.
[3] Cole SP, Bhardwaj G, Gerlach JH, Mackie JE, Grant CE, Almquist KC, et al. Overexpression of a transporter gene in a multidrug-resistant human lung cancer cell line. Science 1992;258:1650–4.
[4] Newman DJ, Cragg GM. Natural products as sources of new drugs over the last 25 years. J Nat Prod 2007;70:461–77.
[5] Cragg GM, Newman DJ, Weiss RB. Coral reefs, forests, and thermal vents: the worldwide exploration of nature for novel antitumor agents. Semin Oncol 1997;24:156–63.
[6] Chang JY, Chang CY, Kuo CC, Chen LT, Wein YS, Kuo YH. Salvinal, a novel microtubule inhibitor isolated from Salvia miltiorrhizae Bunge (Danshen), with antimitotic activity in multidrug-sensitive and -resistant human tumor cells. Mol Pharmacol 2004;65:77–84.
[7] Shiah HS, Lee WS, Juang SH, Hong PC, Lung CC, Chang CJ, et al. Mitochondria-mediated and p53-associated apoptosis induced in human cancer cells by a novel selenophene derivative, D-501036. Biochem Pharmacol 2007;73(March (1)):610–9.
[8] Kuo CC, Hsieh HP, Pan WY, Chen CP, Liou JP, Lee SJ, et al. BPR0L075, a novel synthetic indole compound with antimitotic activity in human cancer cells, exerts effective antitumoral activity *in vivo*. Cancer Res 2004;64:4621–8.
[9] Juang SH, Lung CC, Hsu PC, Hsu KS, Li YC, Hong PC, et al. D-501036, a novel selenophene-based triheterocycle derivative, exhibits potent *in vitro* and *in vivo* antitumoral activity which involves DNA damage and ataxia

telangiectasia-mutated nuclear protein kinase activation. Mol Cancer Ther 2007;6:193–202.
[10] Liou JP, Hsu KS, Kuo CC, Chang CY, Chang JY. A novel oral indoline-sulfonamide agent. N-[1-(4-methoxybenzenesulfonyl)-2,3-dihydro-1H-indol-7-yl]-isonicotinamide (J30), exhibits potent activity against human cancer cells *in vitro* and *in vivo* through the disruption of microtubule. J Pharmacol Exp Ther 2007;323:398–405.
[11] Kuo YH, Chen CH, Lin YL. New lignans from the heartwood of Chamaecyparis obtusa var. formosana. Chem Pharm Bull (Tokyo) 2002;50:978–80.
[12] Chien SC, Chang JY, Kuo CC, Hsieh CC, Yang NS, Kuo YH. Cytotoxic and novel skeleton compounds from the heartwood of Chamaecyparis obtusa var. formosana. Tetrahedron Lett 2007;48:1567–9.
[13] Kuo YH, Chen CH, Chien SC, Lin HC. Novel diterpenes from the heartwood of Chamaecyparis obtusa var. formosana. Chem Pharm Bull (Tokyo) 2004;52:764–6.
[14] Kuo YH, Chen CH, Chien SC, Lin YL. Five new cadinane-type sesquiterpenes from the heartwood of Chamaecyparis obtusa var. formosana. J Nat Prod 2002;65:25–8.
[15] Gaj CL, Anyanwutaku I, Chang YH, Cheng YC. Decreased drug accumulation without increased drug efflux in a novel MRP-overexpressing multidrug-resistant cell line. Biochem Pharmacol 1998;55:1199–211.
[16] Ferguson PJ, Fisher MH, Stephenson J, Li DH, Zhou BS, Cheng YC. Combined modalities of resistance in etoposide-resistant human KB cell lines. Cancer Res 1988;48:5956–64.
[17] Chang JY, Liu JF, Juang SH, Liu TW, Chen LT. Novel mutation of topoisomerase I in rendering cells resistant to camptothecin. Cancer Res 2002;62:3716–21.
[18] Shi Q, Chen K, Morris-Natschke SL, Lee KH. Recent progress in the development of tubulin inhibitors as antimitotic antitumor agents. Curr Pharm Des 1998;4:219–48.
[19] Jordan A, Hadfield JA, Lawrence NJ, McGown AT. Tubulin as a target for anticancer drugs: agents which interact with the mitotic spindle. Med Res Rev 1998;18:259–96.
[20] Islam MN, Iskander MN. Microtubulin binding sites as target for developing anticancer agents. Mini Rev Med Chem 2004;4:1077–104.
[21] Jordan MA, Wilson L. Microtubules as a target for anticancer drugs. Nat Rev Cancer 2004;4:253–65.
[22] Teicher BA. Newer cytotoxic agents: attacking cancer broadly. Clin Cancer Res 2008;14:1610–7.
[23] Dumontet C, Sikic BI. Mechanisms of action of and resistance to antitubulin agents: microtubule dynamics, drug transport, and cell death. J Clin Oncol 1999;17:1061–70.
[24] Chang JY, Yang MF, Chang CY, Chen CM, Kuo CC, Liou JP. 2-Amino and 2′-aminocombretastatin derivatives as potent antimitotic agents. J Med Chem 2006;49:6412–5.
[25] Chang JY, Hsieh HP, Chang CY, Hsu KS, Chiang YF, Chen CM, et al. 7-Aroylaminoindoline-1-sulfonamides as a novel class of potent antitubulin agents. J Med Chem 2006;49:6656–9.
[26] Liou JP, Wu CY, Hsieh HP, Chang CY, Chen CM, Kuo CC, et al. 4- and 5-aroylindoles as novel classes of potent antitubulin agents. J Med Chem 2007;50:4548–52.
[27] Liou JP, Wu ZY, Kuo CC, Chang CY, Lu PY, Chen CM, et al. Discovery of 4-amino and 4-hydroxy-1-aroylindoles as potent tubulin polymerization inhibitors. J Med Chem 2008;51:4351–5.
[28] Chang JY, Hsieh HP, Pan WY, Liou JP, Bey SJ, Chen LT, et al. Dual inhibition of topoisomerase I and tubulin polymerization by BPR0Y007, a novel cytotoxic agent. Biochem Pharmacol 2003;65:2009–19.
[29] Deng L, Tatebe S, Lin-Lee YC, Ishikawa T, Kuo MT. MDR and MRP gene families as cellular determinant factors for resistance to clinical anticancer agents. Cancer Treat Res 2002;112:49–66.
[30] Norbury C, Nurse P. Animal cell cycles and their control. Annu Rev Biochem 1992;61:441–70.
[31] Kumagai A, Dunphy WG. The cdc25 protein controls tyrosine dephosphorylation of the cdc2 protein in a cell-free system. Cell 1991;64:903–14.
[32] King KL, Cidlowski JA. Cell cycle and apoptosis: common pathways to life and death. J Cell Biochem 1995;58:175–80.
[33] Strausfeld U, Labbe JC, Fesquet D, Cavadore JC, Picard A, Sadhu K, et al. Dephosphorylation and activation of a p34cdc2/cyclin B complex *in vitro* by human CDC25 protein. Nature 1991;351:242–5.
[34] Sorger PK, Dobles M, Tournebize R, Hyman AA. Coupling cell division and cell death to microtubule dynamics. Curr Opin Cell Biol 1997;9:807–14.
[35] Downing KH. Structural basis for the interaction of tubulin with proteins and drugs that affect microtubule dynamics. Annu Rev Cell Dev Biol 2000;16:89–111.
[36] Uppuluri S, Knipling L, Sackett DL, Wolff J. Localization of the colchicine-binding site of tubulin. Proc Natl Acad Sci USA 1993;90:11598–602.
[37] Hamel E, Lin CM. Interactions of combretastatin, a new plant-derived antimitotic agent, with tubulin. Biochem Pharmacol 1983;32:3864–7.
[38] Nagle A, Hur W, Gray NS. Antimitotic agents of natural origin. Curr Drug Targets 2006;7:305–26.
[39] Mollinedo F, Gajate C. Microtubules, microtubule-interfering agents and apoptosis. Apoptosis 2003;8:413–50.
[40] Chipuk JE, Green DR. Do inducers of apoptosis trigger caspase-independent cell death? Nat Rev Mol Cell Biol 2005;6:268–75.
[41] Haldar S, Basu A, Croce CM. Bcl2 is the guardian of microtubule integrity. Cancer Res 1997;57:229–33.
[42] Yamamoto K, Ichijo H, Korsmeyer SJ. BCL-2 is phosphorylated and inactivated by an ASK1/Jun N-terminal protein kinase pathway normally activated at G(2)/M. Mol Cell Biol 1999;19:8469–78.
[43] Vitale I, Antoccia A, Cenciarelli C, Crateri P, Meschini S, Arancia G, et al. Combretastatin CA-4 and combretastatin derivative induce mitotic catastrophe dependent on spindle checkpoint and caspase-3 activation in non-small cell lung cancer cells. Apoptosis 2007;12:155–66.
[44] Wang LG, Liu XM, Kreis W, Budman DR. The effect of antimicrotubule agents on signal transduction pathways of apoptosis: a review. Cancer Chemother Pharmacol 1999;44:355–61.
[45] Srivastava RK, Srivastava AR, Korsmeyer SJ, Nesterova M, Cho-Chung YS, Longo DL. Involvement of microtubules in the regulation of Bcl2 phosphorylation and apoptosis through cyclic AMP-dependent protein kinase. Mol Cell Biol 1998;18:3509–17.
[46] Blagosklonny MV, Giannakakou P, el-Deiry WS, Kingston DG, Higgs PI, Neckers L, et al. Raf-1/bcl-2 phosphorylation: a step from microtubule damage to cell death. Cancer Res 1997;57:130–5.
[47] Fecker LF, Geilen CC, Hossini AM, Schwarz C, Fechner H, Bartlett DL, et al. Selective induction of apoptosis in melanoma cells by tyrosinase promoter-controlled CD95 ligand overexpression. J Invest Dermatol 2005;124:221–8.
[48] Imai T, Adachi S, Nishijo K, Ohgushi M, Okada M, Yasumi T, et al. FR901228 induces tumor regression associated with induction of Fas ligand and activation of Fas signaling in human osteosarcoma cells. Oncogene 2003;22:9231–42.
[49] Lu B, Wang L, Stehlik C, Medan D, Huang C, Hu S, et al. Phosphatidylinositol 3-kinase/Akt positively regulates Fas (CD95)-mediated apoptosis in epidermal Cl41 cells. J Immunol 2006;176:6785–93.
[50] Yamamoto K, Katayose Y, Suzuki M, Unno M, Sasaki T, Mizuma M, et al. Adenovirus expressing p27KIP1 induces apoptosis against cholangiocarcinoma cells by triggering Fas ligand on the cell surface. Hepatogastroenterology 2003;50(November-December):1847–53.
[51] Torgler R, Jakob S, Ontsouka E, Nachbur U, Mueller C, Green DR, et al. Regulation of activation-induced Fas (CD95/Apo-1) ligand expression in T cells by the cyclin B1/Cdk1 complex. J Biol Chem 2004;279:37334–42.